In this page are summarized a few recent results detailed in the publications accessible HERE (Dr Philippe HUETZ).

THE POTASSIUM CHANNEL KcsA: MOLECULAR DYNAMICS and AB INITIO STUDIES

- new insights with partial charge calculations -

- ions and water behaviour -

PARTIAL CHARGE CALCULATIONS ON THE LIPID DIOCTADECYLAMINE ($(C_{18}H_{37})_2NH$) aroused suspicions !

PARTIAL CHARGES

The charge is defined by the following integral:

$$q = \int_{r_{min}}^{r_{max}} n(r)dr$$

n(r): electronic density

- Partial charge is not an observable
- The notion of charge becomes difficult at the nanometric scale !

If one restricts the domain of observation of the electronic density, the charge will take a distinctive relief. Moreover, it will be dependent on the conformation, through the interplay of wave functions overlap.

Amber charges: non polarizable model (empirical)

Charge calculations for different biomolecular systems according to the Merz-Kollman-Singh (MK) scheme:

atomic charges are fitted to reproduce the molecular electrostatic potential (MEP) on a certain number of points on a grid consisting of several layers around the molecule

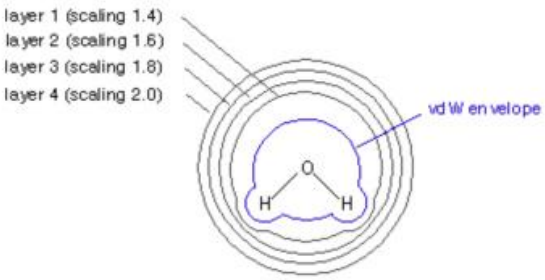

These layers are defined at distances between 1.4 and 2.0 times van der Waals radius.

Ab initio calculations of the partial charge distribution on the lipid model **DIOCTADECYLAMINE** (DODA) were performed using the suite of programs Gaussian 98 (**Chem. Phys. Lett. 380 (2003) 424-434**). Chosen level of theory: HF/6-31G(2d). Three distinct conformations were used for charge calculation, after energy optimization: one completely stretched (DODA-str), one slightly twisted (DODA-tw1) and one strongly twisted (DODA-tw2). They are represented here (left):

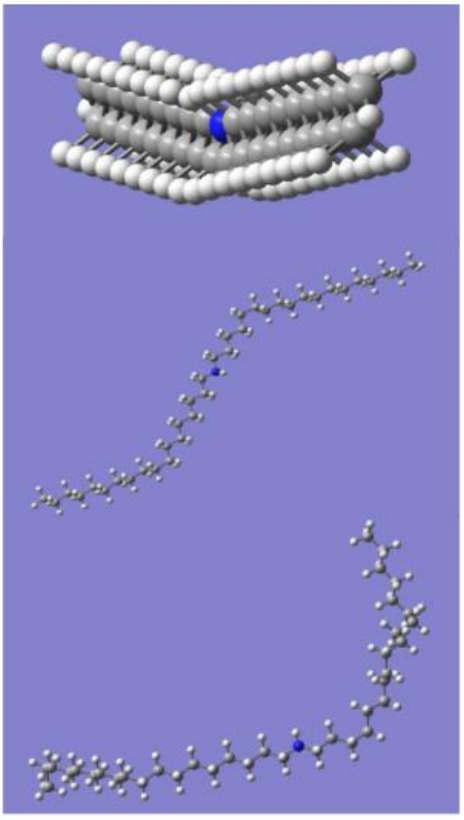

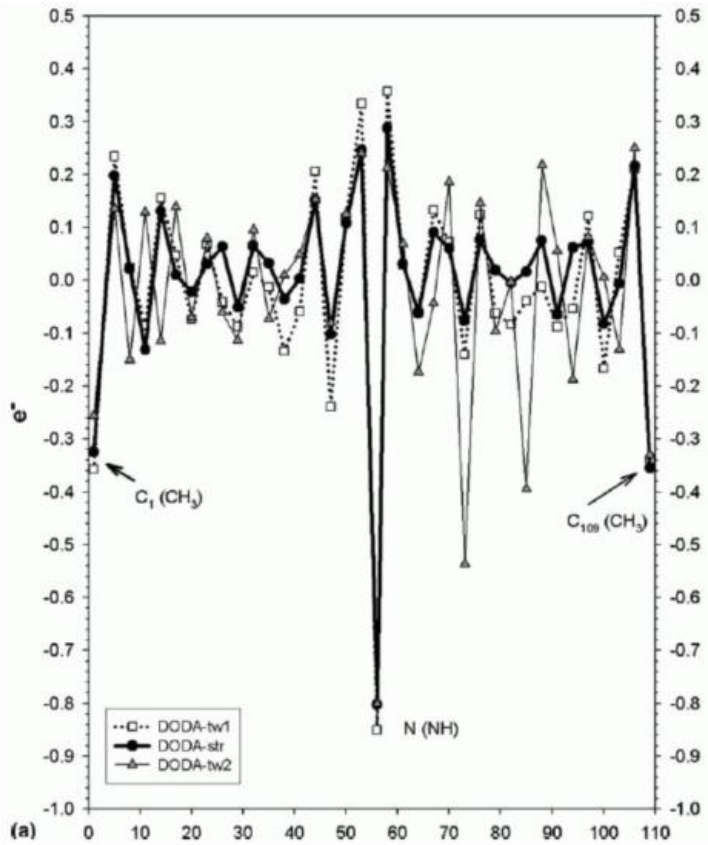

Calculations were done as well in gas phase as in presence of a solvent (dielectric continuum of Tomasi and coworkers or Langevin dipoles of Florián and Warshel). Again we focused on atomic charges derived from the electrostatic potential according to the Merz-Kollman-Singh scheme. After comparison of the charges obtained at different levels of theory on the stretched

form of DODA, we showed that gas phase charges were sufficient to represent what appeared to be an intrinsic property of the lipid, independently from the solvent.

The graph (right) shows the three superimposed curves corresponding to the different situations. Charges on each carbon are shown, following the chain from left to right, nitrogen in the center. We see that in the most coiled, unordered parts of the aliphatic chains, significant partial charge fluctuations occur, one carbon charge value getting close to the nitrogen one ! A periodic behaviour of these charges can also be noticed. Thus, differences in partial charges are enormous and depend on conformation.

For proteins for instance, this work shows how important it would be to develop force fields with conformation-dependent charges to correctly describe their dynamics.

THE VOLTAGE-GATED POTASSIUM CHANNEL KcsA (2.0 Å resolution structure)

This work has represented an essential step for modelling KcsA, a potassium channel whose 3D structure has been recently awarded by a Nobel price.

The voltage-gated KcsA channel is the K^+ channel from *Streptomyces lividans*, similar in structure to other K^+ channels, e.g. in vertebrates. It is a highly selective tetrameric protein machinary devoted to potassium ions directional transfer through the cell membrane. This function is essential for e.g. neuron electrical signals generation or heart beat. It is yet difficult to understand how such a mechanism can be as much efficient (flow of ca. 10^7 K^+ ions per channel per s) and selective (about 1 Na^+ ion for at least 10^3 K^+ transported). The recent X-ray structure of a procaryotic KcsA channel shed light on the molecular bases of this process, as well as different molecular dynamics (MD) simulations and theoretical electrostatics and energetics studies. The protein switches between an open and a closed structure, **where only the closed one is known precisely, the open one being modeled from site-directed spin labeling and electron paramagnetic resonance spectroscopy data or computational conformation analyses**. Three main regions participate to the channel K^+ diffusion (see figure): the selectivity filter (F) at the outermost part of the cell membrane, a water-filled cavity (C) half way across the membrane, followed by the gate region (G), a vestibule at the innermost part covered with hydrophobic residues.

KcsA IN ITS LIPIDIC ENVIRONMENT

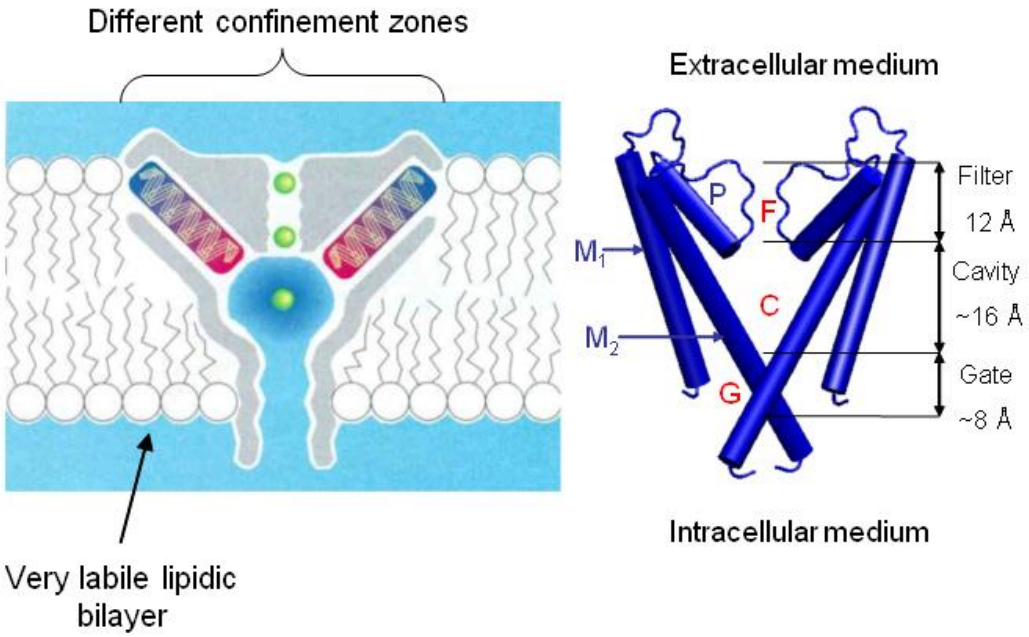

We have seen that the atomic charges may fluctuate enormously at the level of the lipids,
what about in the membrane channels ?

Building the system

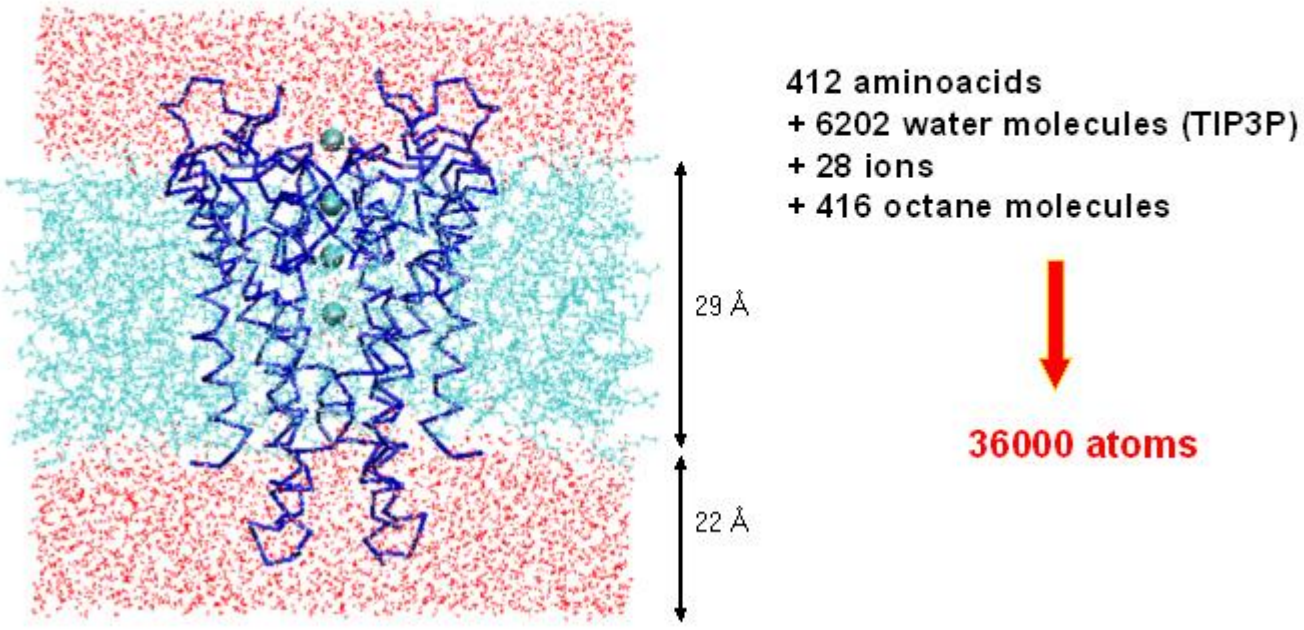

Molecular Dynamics (MD): relaxation till equilibrium

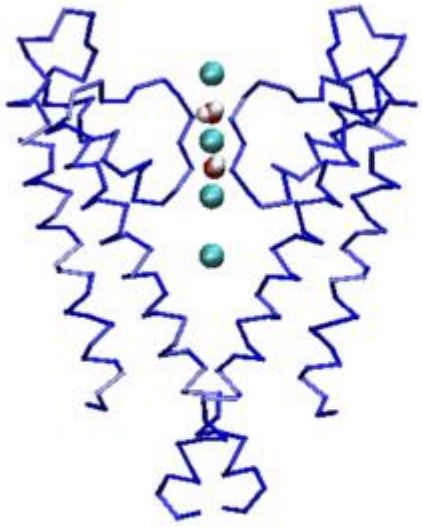

KWKWK... K

= starting sequence in MD

Experimentally: 6 sites occupied either by a water molecule or by a K^+ ion

K W sequence chosen to test maximum pore occupancy

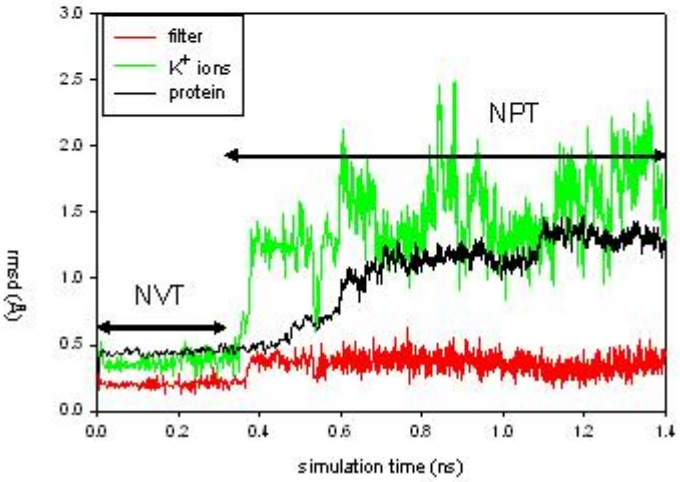

We have chosen in a first stage to study more specifically **the selectivity filter of KcsA**, located on the extracellular matrix side. Ab initio calculations of partial charges were performed for two specific conformations of the selectivity filter, cut out along a height of 4 aminoacids (**Chem. Phys. Lett. 397 (2004) 510-515**).

KcsA selectivity filter: ab initio study

(truncated structure TVGY - 304 atoms)

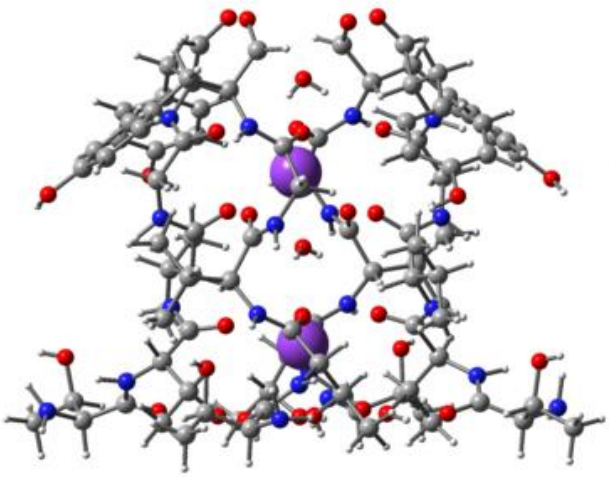

Mean configuration over 600 ps MD

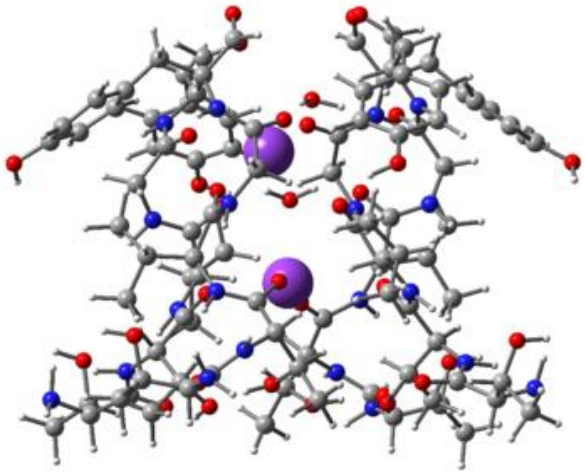

Specific snapshot in same trajectory, suspected to be at the origin of the 'knock-on' mechanism

The four α-helices point towards the central pocket and are lined up with carbonyls of the peptide bonds, disposed four by four in successive planes, in between which the K^+ ions are stabilized in alternation with single water molecules (sites numbered 1 to 4, from top to bottom). The second configuration is extreme, suspected to be at the origin of a mechanism initiating diffusion of the ions, the so-called knock-on mechanism.

The central result of the charge calculation is presented in the following table:

Results: MK charges
HF/6-31G(d) – Gaussian 03

	$O(W_1)$-K_2	K_2-$O(W_3)$	$O(W_3)$-K_4	K_2-K_4
600 ps average geometry (C1)	3.10 **O: -0.767**	2.40 **O: -0.816**	3.05	5.35 **K_2: 0.755 - K_4: 0.687**
Specific snapshot (C2)	2.68 **O: -0.876**	2.51 **O: -0.948**	2.79	4.30 **K_2: 0.871 - K_4: 0.875**

Center to center distances (Å) between the oxygen atom of the water molecules and the K^+ ions of sites 1 to 4 of the KcsA selectivity filter (first data). Second data (bold): MK partial charges in units of electron charge (e^-) for $O(H_2O)$ or K^+ of the corresponding sites.

It can be seen that the oxygens of the water molecules carry charges close to the values of a TIP3P model, whereas for the potassium ions, the charge is far from being equal to 1, the value usually attributed in classical MD force fields, and on the contrary can decrease up to about 0.69 e^-, in this specific case !

THIS RESULT IS CRUCIAL FOR A BETTER UNDERSTANDING OF THE MECHANISTICS OF K^+ CHANNELS IN PARTICULAR AND IONIC CHANNELS IN GENERAL.

We then had a look at the isopotential-energy surfaces (quantum calculations) for a unit probe charge (+1) exploring the KcsA filter (configuration averaged over 600 ps MD) empty or filled with the water-potassium ion-water-potassium ion sequence.

Truncated selectivity filter: isopotential-energy surfaces

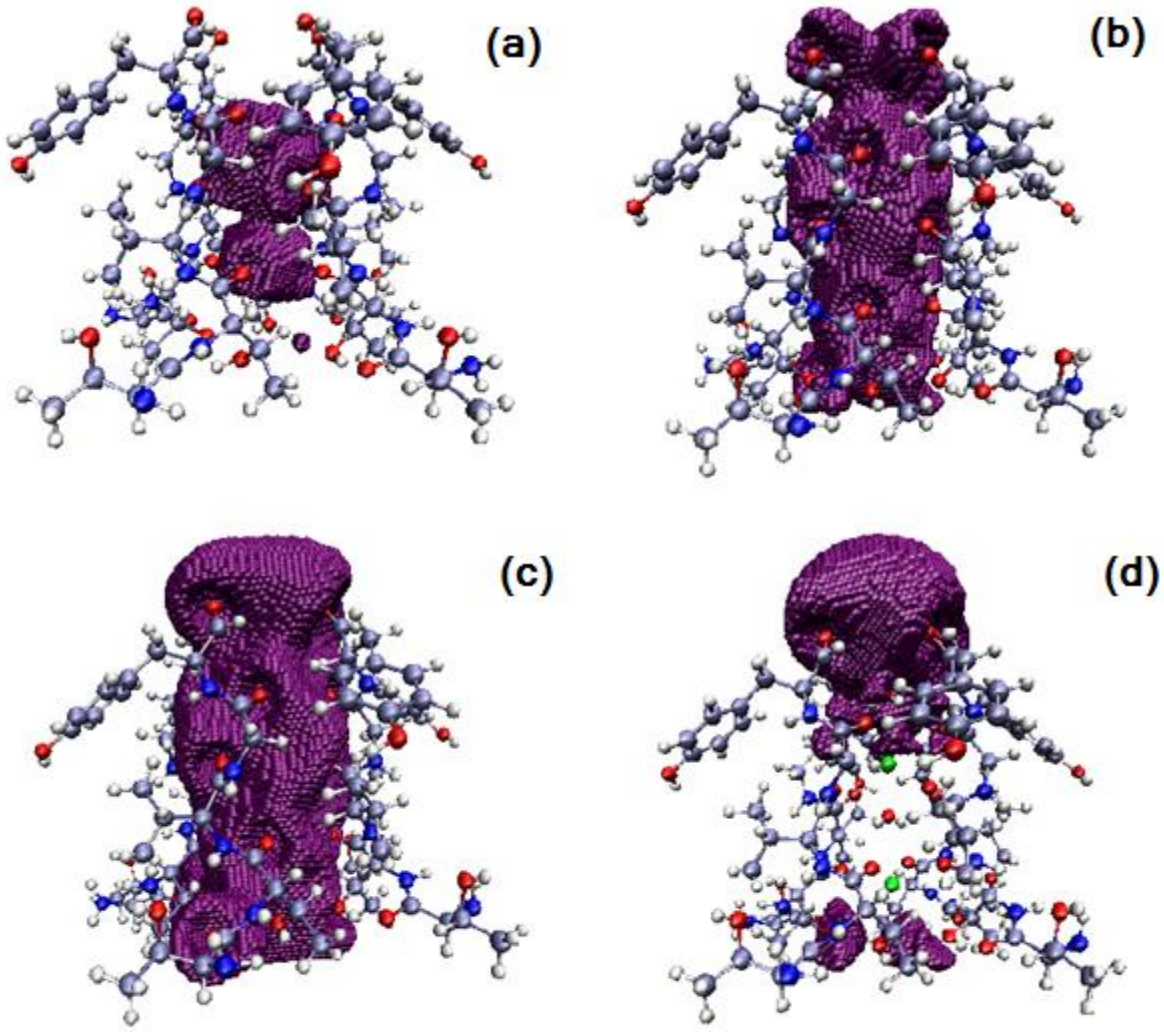

(a) -120 **(b)** -80 **(c)** -50 kcal.mol^{-1} : filter empty
(d) 20 kcal.mol^{-1}: with sequence WKWK

Depending on the energy, the different binding sites of as well the inner part of the filter as, at higher energy the one at the outer mouth of the channel (larger attractive zone) were found, in agreement with the literature experimental and numerical results. Due to the truncation of the protein structure, the most external extracellular site and the cavity site (intrinsically due to the water-filled cavity) cannot be observed. The filter part of the protein, by itself, is thus responsible for the occurrence of five sites. When the filter is occupied by the sequence WKWK, due to large repulsive interactions (both electrostatic for the K^+ ions of the sequence and steric for the K^+ and W), the probe charge can only explore very limited regions of the filter (d). The outermost protuberance is there again, i.e. the filter mouth can still be occupied by a K^+ ion (S_0 site), even though the inner part of the filter is filled.

Partial charges: an explanation for KcsA selectivity/conductivity ?

May partial charges bring an explanation for the 1000 to 10000 times greater selectivity of KcsA for potassium than sodium ? We compared binding energies for K^+ and Na^+ (J. Chem. Phys. 124 (2006) 044703).

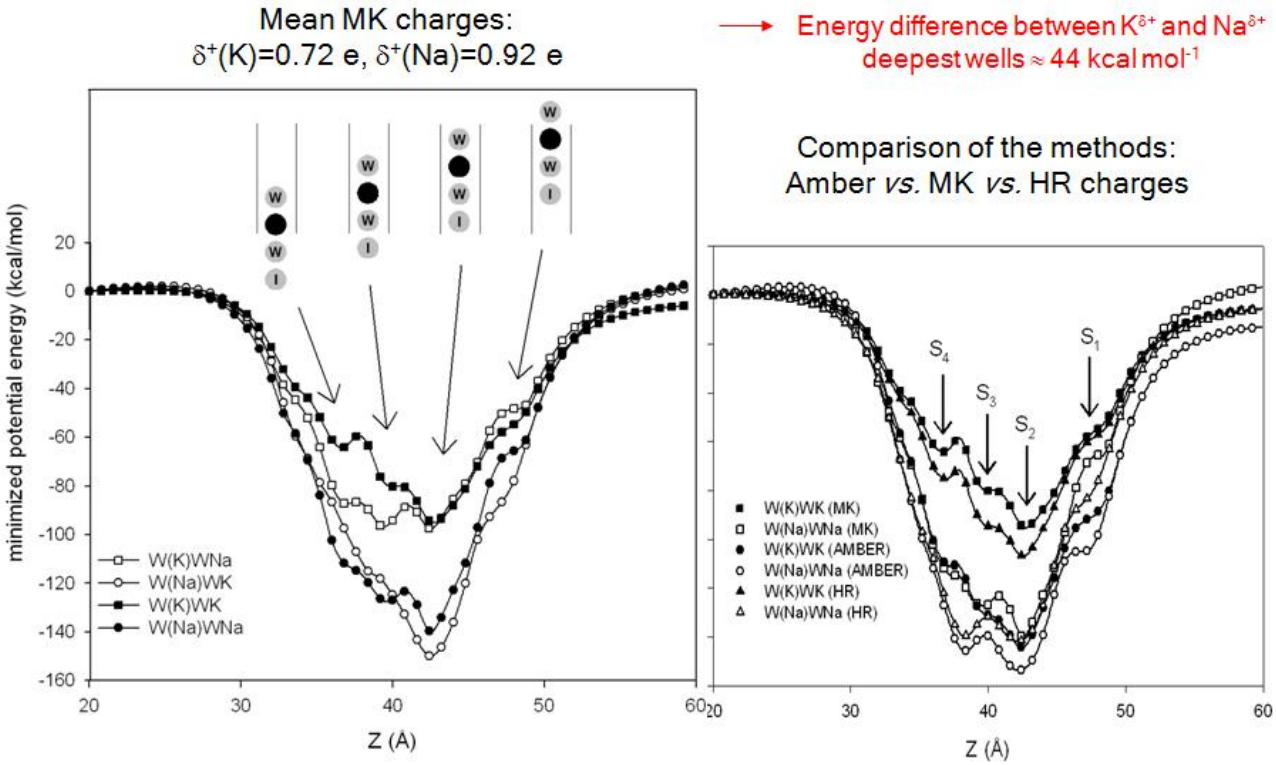

Firstly we compared different methods (right graph):

- AMBER empirical force-field, where K^+ and Na^+ charges are +1,
- Merz-Kollman charges (MK, see above),
- and a method developed by Hinsen and Roux (HR), which checks for possible artefacts in charge calculation.

Lennard-Jones parameters were included.

The potential energy experienced by $K^{\delta+}$ or $Na^{\delta+}$ ions at position 2 in WKWK or WNaWNa rigid sequences exploring the empty filter along the Z axis (perpendicular minimization) is shown, with for MK and HR methods the average values of ion and water oxygen charges obtained for each sequence in each method. For the sodium, K^+ were replaced by Na^+ in the same configuration. AMBER corresponding curves are shown as references. The four sites corresponding to the WKWK electrostatic potential (ESP) curves are indicated. We see that the overall scheme of the site locations is not fundamentally changed, as expected with just a difference in the charge values. By contrast and with ESP charges, large energy shifts are obtained when compared to curves drawn with AMBER charges, especially for potassium.

Secondly we compare the energy curves calculated in the MK scheme for the four sequences WKWK, WNaWK, WKWNa, and WNaWNa (left graph).

RESULTS:

- Replacing K by Na ion in position 4 of the sequence does not strongly modify the depth of the minimum well;
- The most stable site is S_2;
- The energy required by the Na ion at position 2 in the sequence to escape from the filter is always larger than for the K ion at the same position, whatever the second ion is in the sequence. The energy difference is around 44 kcal mol^{-1}.

STATIC MODEL:

P.H. Nelson's model of permeation : concerted-motion mechanism for ion translocation within a single-file ion channel (simplified, static analysis)

$P_{Na/K}(V=0)$: ~ proportional to $\exp(-\Delta\Delta E/kT)$

- selectivity ratio (ratio of the fluxes J_{Na}/J_K)
- energy difference for the dissociation of $K^{\delta+}$ and $Na^{\delta+}$ ions
- at equilibrium

When $\Delta\Delta E = 44$ kcal mol^{-1} => unrealistic $P_{Na/K}$ value (10^{-32})
$\Delta\Delta E$ should be < 10 kcal mol^{-1} within Nelson's model
Bulk hydration Na/K energy difference ≈ 18 kcal mol^{-1}
Na/K hydration entropic contribution should be ~ identical (Kebarle)
=> $\Delta\Delta E = 26$ kcal mol^{-1} , still overestimated

BUT: - hydration takes place in confined water (cavity),
- neglect of the entropic term difference in $\Delta\Delta E$ Na/K

DYNAMIC MODEL:

Franck-Condon-type approach (dynamic analysis, knock-on condition with distance contraction of 0.75 Å of the ion closest to the cavity)

→ the energy excess due to distance contraction is completely used by each cation to reach the final state (escape from the filter)

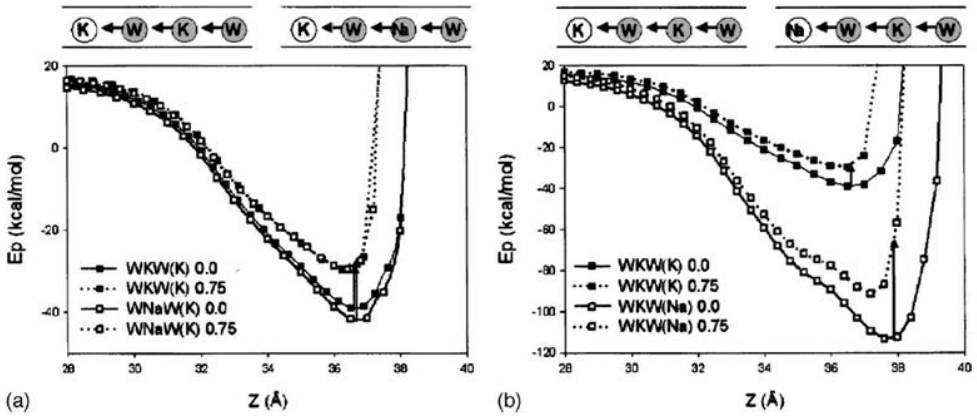

Behavior of the potential seen by the ion in site S_4

a) influence of S_2 ion on the escape of K_4 is small (≈ 3 kcal mol^{-1})
b) significant ΔEp between Na_4 and K_4 escapes from the filter : decrease from 75 (no distance contraction) to 39 kcal mol^{-1} (knock-on)

=> after hydration contribution correction, effective energy difference of 21 kcal mol^{-1}

CONCLUSION : Although the values obtained here for ΔΔE in both situations correspond to a gross estimate, this demonstrates in a qualitative way that considering partial charge (and not unitary charge) for the cations, together with fluctuations of their positions in the sequence (i.e., differences in repulsion strengths), could be an important phenomenon to discriminate the behavior of the two cation species in the filter.

Average dipoles (D) for the 2 X 4 carbonyl groups of the residues located around S_2

	Val76 C=O	Gly77 C=O
AMBER	3.41	3.43
MK (empty)	4.12	3.15
MK (*WK*W*K*)	4.23	3.45
MK (*WNa*W*Na*)	4.48	3.54

Noskov et al. : - dipole between 2.5 and 4.5 D => filter selects K^+ over Na^+
- would become selective for Na^+ if ≈ 7 D

⇨ consistent with selectivity of potassium over sodium

ROLE OF WATER MOLECULES IN KcsA BY MOLECULAR DYNAMICS CALCULATIONS

In a nanometric confined medium, water molecules behave completely differently compared to a bulk medium. For instance the degree of order, with formation of distinct layers of molecules parallel to the surfaces, the dielectric constant of the solvent which, in turn, influences the effective electrostatic field within the liquid, a decrease of polarization, a slowing of the rate of relaxation of water molecules, are changes which have been observed.

For the KcsA molecule, the density of bulk water in the extra- and intracellular sides was fixed to 1, while the density of water molecules in the cavity was determined by evaluating the Connolly surface. As a consequence a bulk water molecule, which occupies on average a volume of 30 $Å^3$ at 300 K, has its mobility appreciably reduced in the cavity. This is correlated to a strong increase in water density. The cavity could thus contain between 30 and 40 water molecules. The fluctuations of this number initially optimized in the closed state of KcsA were studied during the gating of the channel. We tried to elucidate the correlation between the motions of the K^+ ions located in the cavity with the orientation of the water molecules in the closed and open structures.

A model of the open structure was built combining the C_α known skeleton positions of the open structure derived from EPR experiments and the well-defined closed structure modeled on the basis of X-ray data (targeted MD).

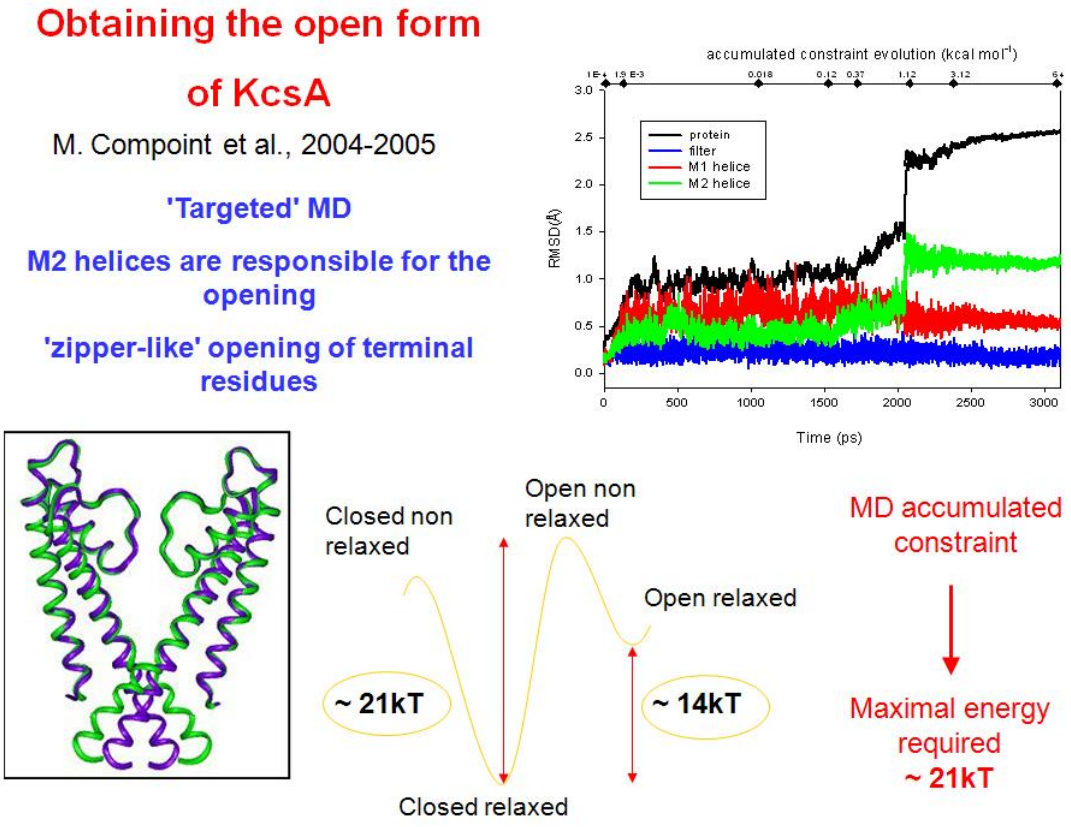

INVESTIGATIONS :

- MD using AMBER 6 force fields (1 fs steps, H_2O TIP3P) on closed and open structures, including sequence KWKWK…K ;
- Follow-up of water molecules and K^+ ions over 3.5 ns (closed) and 1.5 ns (open) simulation time (300 K, structures relaxed) ;
- Follow-up of dipole moments μ of cavity water molecules along x, y and z of trajectories ; calculation of mean μ_z ;
- Dipole moment μ_z of water molecules as a function of K^+ position in the cavity.

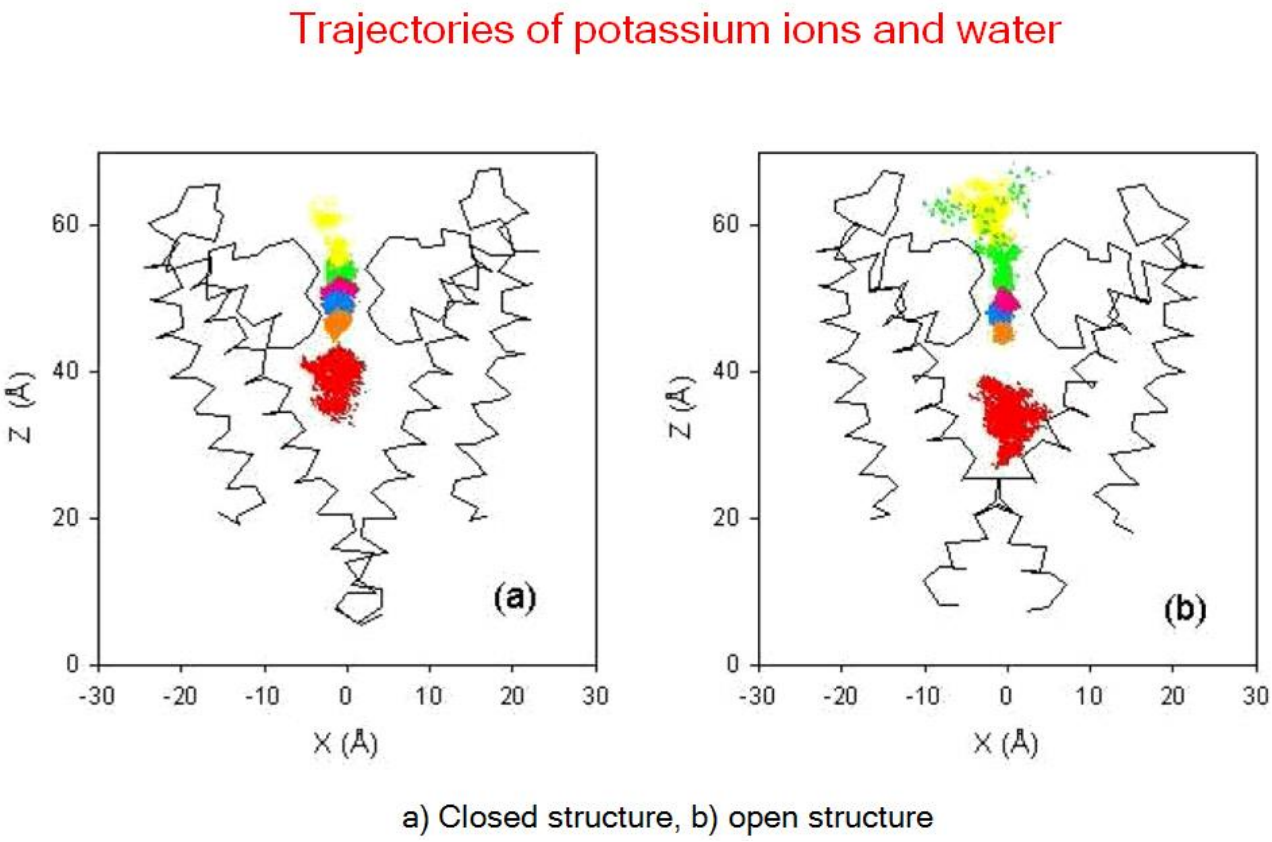

a) Closed structure, b) open structure

This figure shows the trajectories of the centers of mass of the K^+ ions and of the water molecules in the KWKWK. . .K sequence observed in the relaxed closed (a) and open (b) structures during 3.6 and 1.6 ns of the MD run, respectively. We see that i) the species located in the filter are strongly bound to the protein, ii) the spheres belonging to the trajectories of two adjacent species overlap (the atoms move in the filter in a concerted manner), iii) the K_{cav} ion undergoes much larger motions and is located closer to the gate entrance in the open state, where iv) an escape of the species from the pore can also be noticed.

Potential energy profiles (Phys. Chem. Chem. Phys. 7 (2005) 4138-4145) : potential energy felt by a K^{+1} ion along the closed KcsA structure.

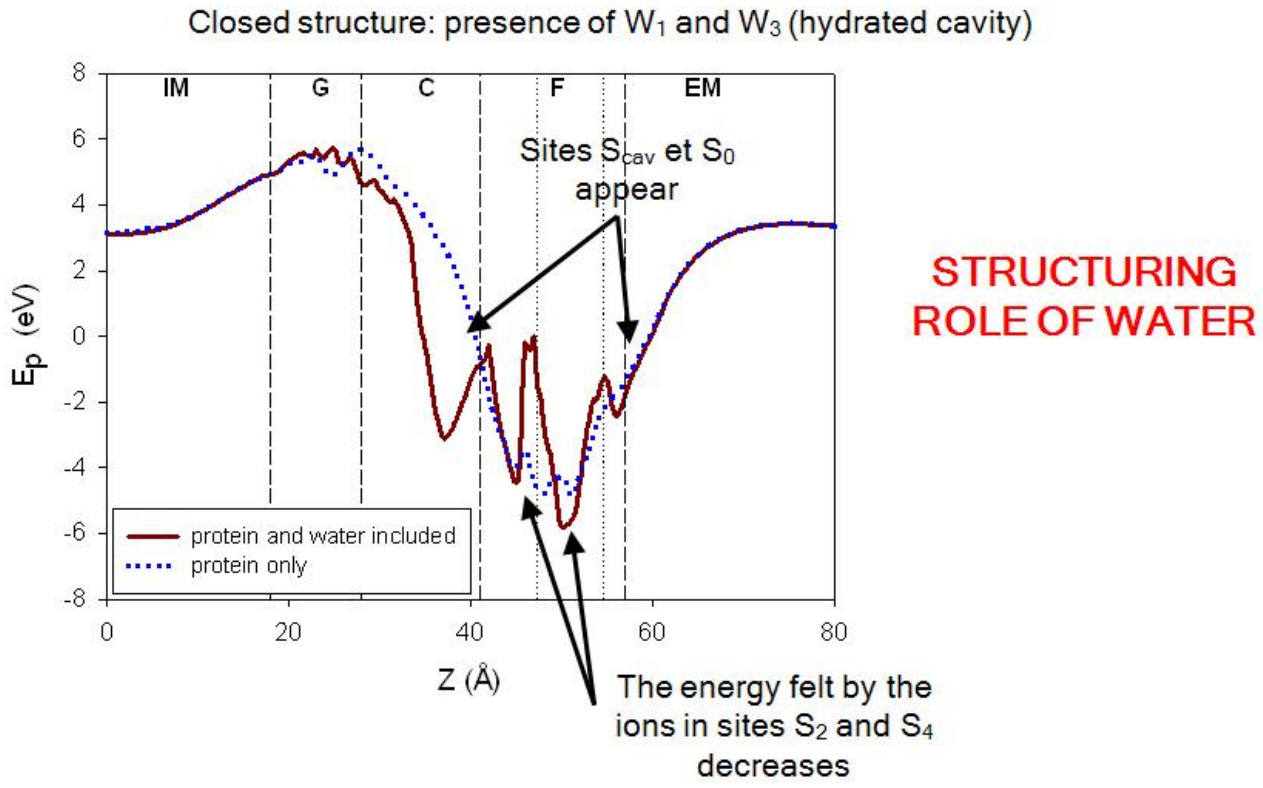

IM/EM: Intra/Extracellular Medium, G: Gate, C: Cavity, F: Filter.

The dotted line corresponds to the energy profile obtained when the filter is empty, whereas the full line to the case where the two water molecules of the filter are present (cavity hydrated also). We clearly see that **the regions where the K^+ ions reside preferentially are more pronounced, whereas two other potassium preferential sites appear**, one at the entrance of the selectivity filter on the EM side and the other inside the cavity, close to the filter entrance. This result is very important and demonstrates the structuring role of water for this biological system.

We also analyzed the behavior of the cavity water dipole in relation with the movement of the potassium ion in the cavity.

Water: dynamic element of the cavity

a) Closed form b) open form

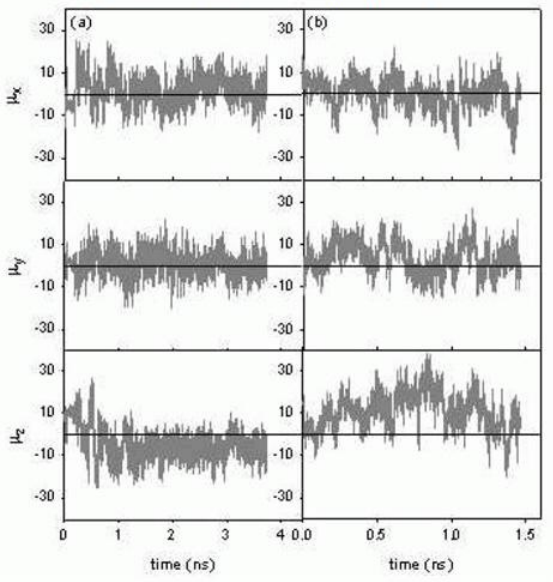

Mean value ~ 0

Tends toward mean finite values: ± ~10 Debye

Induced electric field is fluctuating more in the open form

μ x, y and z componants (geometric sum of all individual H_2O dipoles)

The dipole of water follows the movement of the potassium ion in the cavity !

Position of K_{cav} along z

μ_z H_2O total

μ_z *vs.* K_{cav} (center of mass)

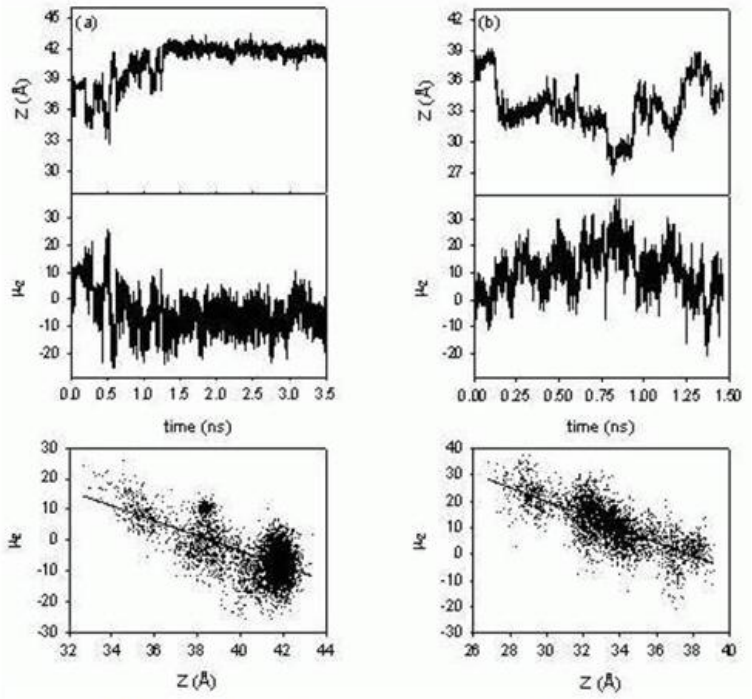

Closed form

Open form

In this figure is shown the movement of the K^+ ion along the z axis of the cavity in the closed and open forms of the channel, during respective relaxation times of 3.5 and 1.5 ns of MD. Superimposed the geometric sum of the z component (i.e. along the pore axis) of the cavity water molecules' dipole moment. The **linear behavior of the bottom curves (μ_z as a function of K_{cav} z position)** demonstrates the fact that these two quantities evolve in a concerted manner. The denser clouds (-10 and +10 Debye) correspond to the preferential positions of K^+ in the cavity, in the closed form near the filter entrance, and in the open form near the gate entrance. The deviations with respect to the linear behavior are due to large fluctuations of the water molecule orientations.

Water molecules have thus 2 distinct characteristic times: one intrinsic characteristic time of the order of the **picosecond (rotation)**, and another of the order of the **nanosecond**, given that the water molecule follows the ion dynamics.

Extreme situations in closed and open forms: μ_z inversion

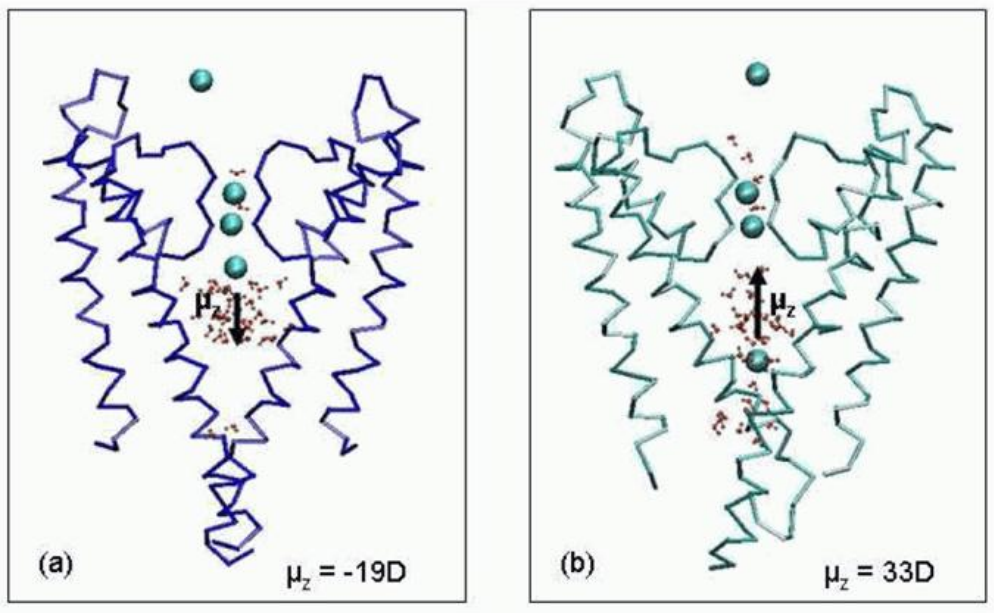

Confined nanometric medium *vs.* liquid medium

▼

very different behavior of water

a) Closed form, b) open form

CHEMICAL REACTIVITY AS A TOOL TO STUDY CARCINOGENICITY

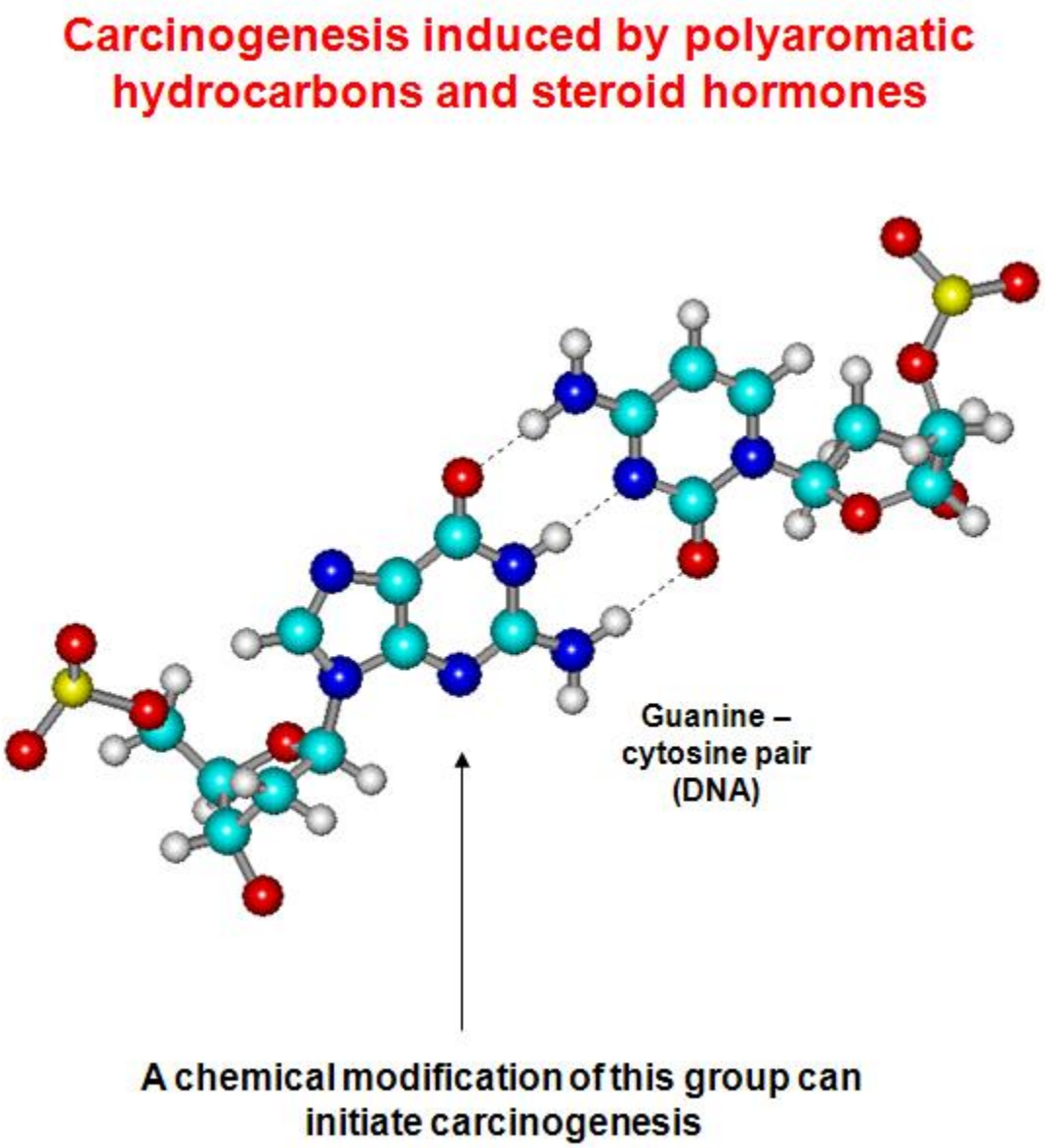

Benzo[*a*]pyrene $\xrightarrow{\text{P450...}}$ Benzo[*a*]pyrene diol epoxide (BPDE) $\xrightarrow{\text{guanine}}$ Guanine Adduct

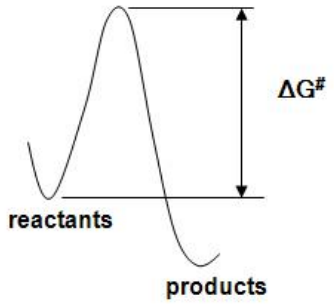

$$k = \frac{k_B T}{h} \cdot e^{-\Delta G^{\#} / k_B T}$$

One to one correspondence between free energy of activation $\Delta G^{\#}$ and rate constant k of the reaction

HYPOTHESIS: ACTIVATION ENERGY of the chemical reaction between the ultimate carcinogen BPDE and guanine (or adenine) is a MESURE OF CARCINOGENICITY

Reaction between a polyphenol and an ultimate carcinogen

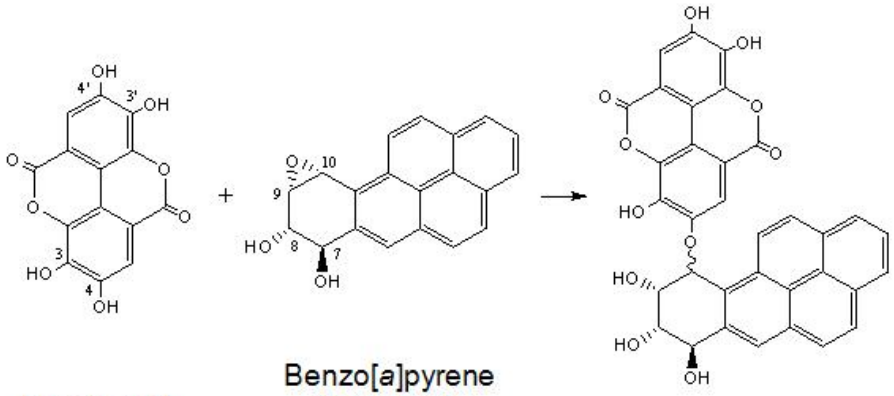

Ellagic acid (EA)

Benzo[*a*]pyrene diol epoxide (BPDE)

cis or *trans* adduct

raspberries
red wine

cigarette smoke
vehicle exhausts

Reaction between ellagic acid and BPDE: determination of transition state B3LYP/6-31G(d)

The transition state was calculated by varying the reaction coordinate in a systematic way

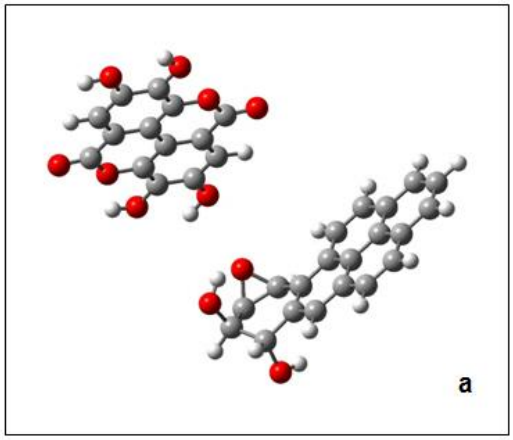

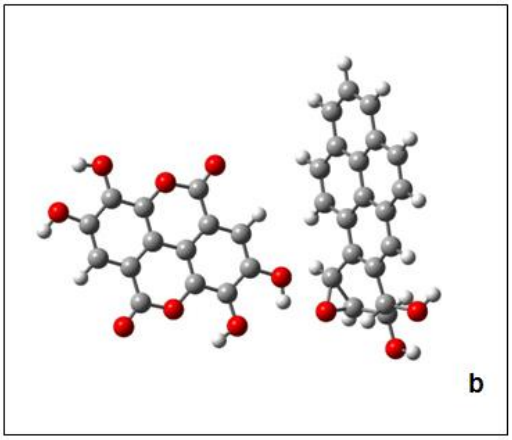

Reactants (a) and transition state (b)
Left: EA, right: BPDE
Optimized structures

TWO SOLVATION MODELS USED

- PCM: Polarizable Continuum Model (J. Tomasi, V. Barone *et al.*)

The solute, whose limits are defined by a realistic cavity shape (interlocking spheres surrounding each atom), is immersed in a dielectric continuum →

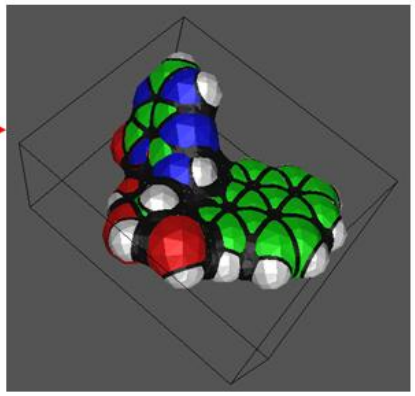

- LD: Langevin Dipoles model (J. Florian et A. Warshel)

→ the solvent is approximated by polarizable dipoles fixed on a cubic lattice
→ the solute, described by a set of point charges, is transferred from the gas phase to the grid of LD (298 K)
→ 50 times displacement of the solute => thermal averaging

RESULTS [J. Chem. Inf. Model. 45 (6) (2005) 1564-1570**] :**

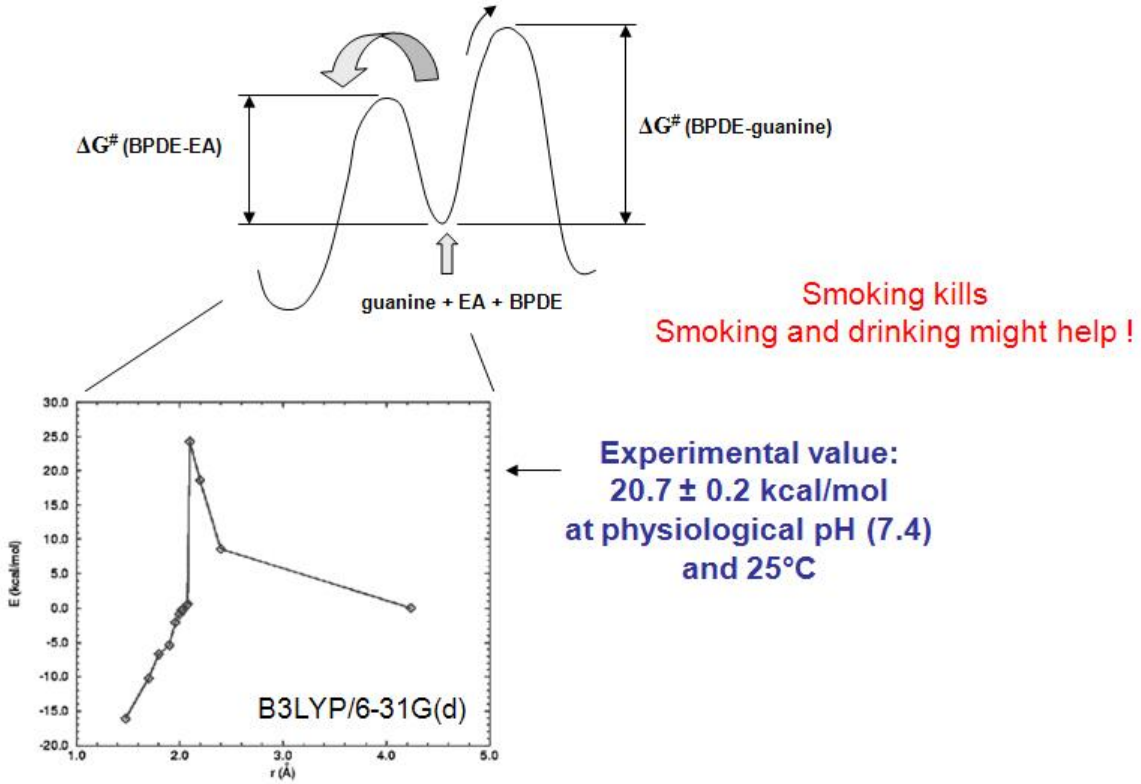

The calculated BPDE/ellagic acid reaction free energy of activation is found to be in decent agreement with experimental data.

LINEAR FREE ENERGY RELATIONSHIPS

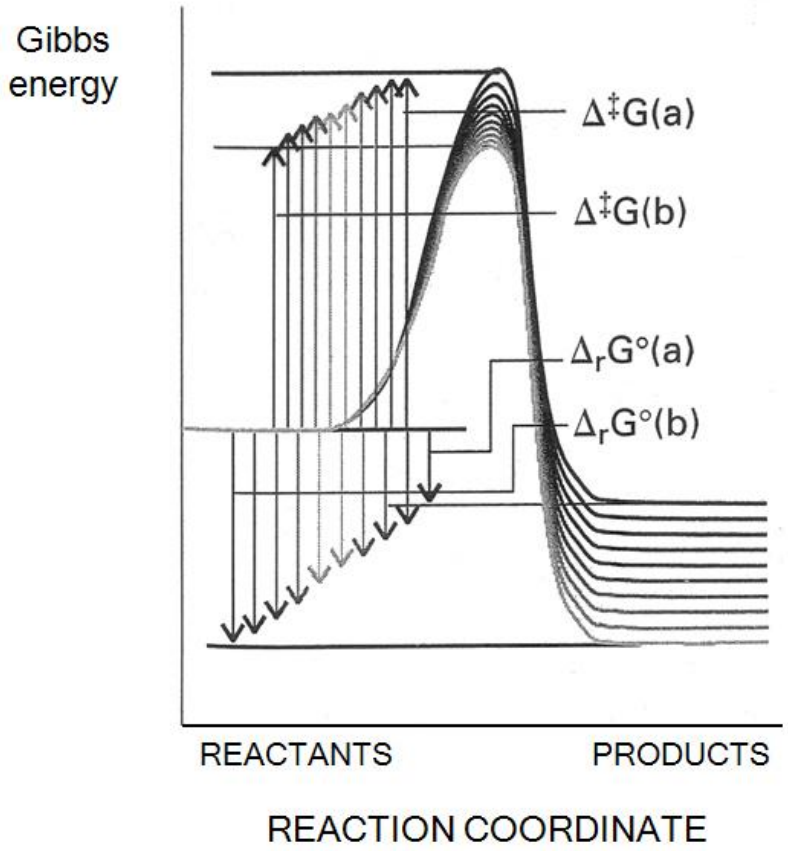

approximatively linear correlation between $\Delta^{\ddagger}G$ (Gibbs activation energy) and $\Delta_rG°$ (reaction free energy)

↓

when analogous structures of the reactants and products and analogous reaction mechanisms

The linear free energy relation is a method of choice to estimate the activation free energy. **The method is empirical and states that in a series of chemical reactions involving similar reactants and having the same mechanism, the reaction with the most favorable reaction free energy will have the lowest free energy of activation.** The rationale behind this is that if one approximates reactant and product free energy hypersurface wells with parabolas, they are expected to have about the same curvatures since we are dealing with similar species. Clearly, the point of their intersection will be lower if the product parabola is lower, giving rise to lower activation free energy for the reaction.

EXAMPLE OF TWO HORMONES: OESTRADIOL AND ESTRONE.

A certain class of procarcinogens is inherent to the human body. This includes steroid hormones that have a partial aromatic structure. Carcinogenesis associated with this class of compounds is called endogeneous, and indeed hormonal carcinogenesis is believed to be responsible for a number of cancers, such as ovary, uterus, mammary gland, and prostate. In particular, a serious controversy is at its height with regard to the inherent risks of **hormone replacement therapy and estrogens' link to breast cancer** (Women's Health Initiative, Million Women Study). As is the case for polyaromatic hydrocarbons, hormones themselves are not carcinogenic, but, aside from an effect which could result from binding to their nuclear receptors, they have to be activated to reactive metabolites to be cancer initiators. Indeed,

endogenous estrogen metabolites, through catechol estrogens formation, have been shown to exhibit genotoxic properties which can lead to carcinogenic DNA mutations.

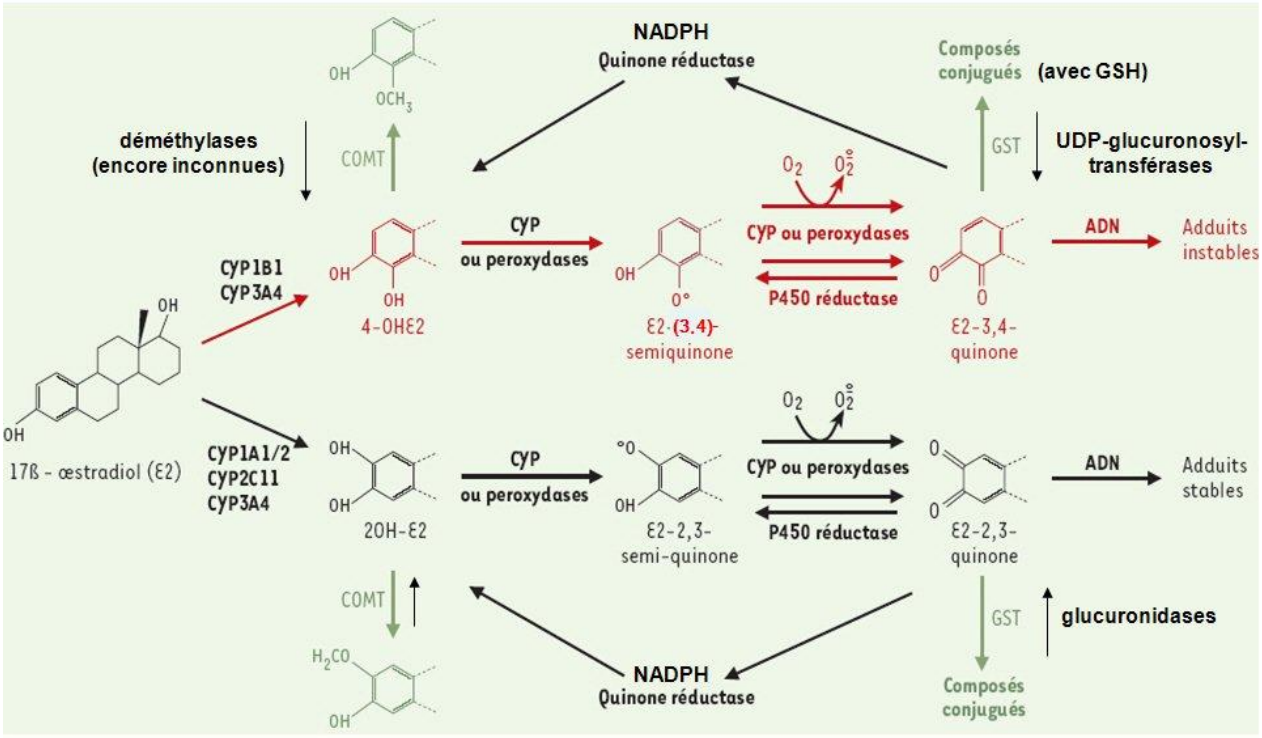

ESTRADIOL METABOLIC PATHS

Application of Linear Free Energy Relationships (LFER)

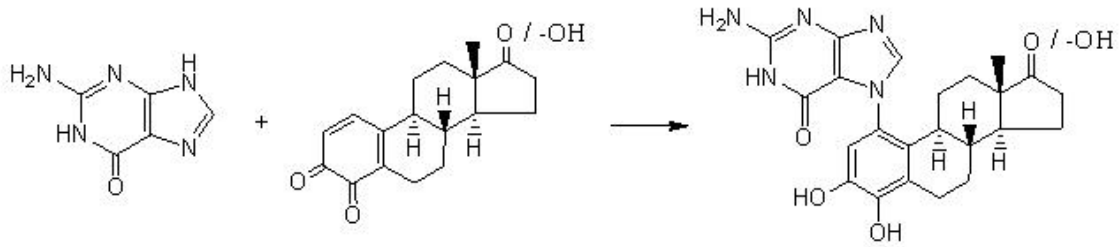

Reaction between estradiol and estrone 3,4-quinones ultimate carcinogens and guanine,
following a Michael reaction mechanism

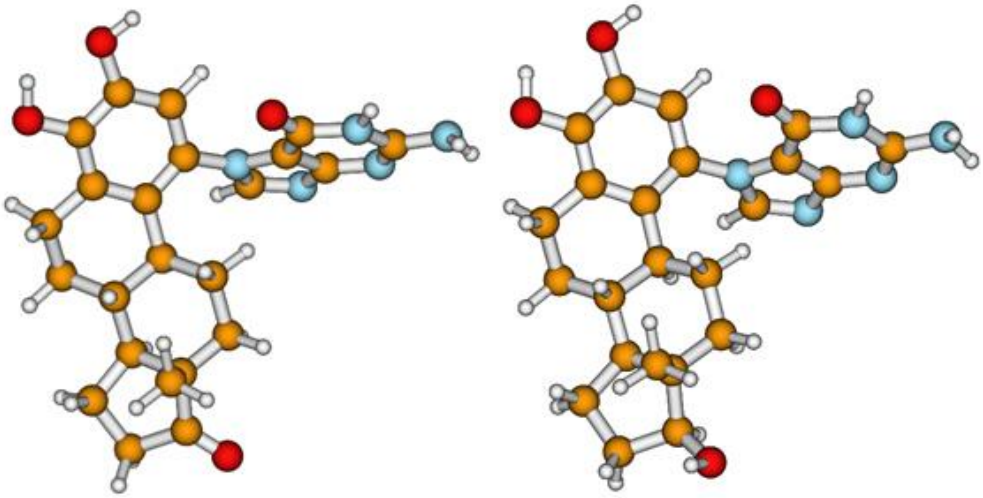

Structure of DFT optimized adducts

RESULTS

Ph. HUETZ *et al.*, J. Chem. Inf. Comput. Sci. 44 (2004) 310-314

	$\Delta E^{(a)}$	$\Delta ZPE^{(b)}$	$\Delta G_{hydr}^{(c)}$	$\Delta G_{hydr}^{(d)}$	$\Delta G_{hydr}^{(e)}$	$\Delta G_{react}^{(f)}$
E_1-3,4-Q	-19.19	2.06	10.96	10.97	15.64	-1.49
E_2-3,4-Q	-18.96	2.17	11.40	10.93	15.17	-1.62

Free energy and free energy components for reactions between estron and estradiol in their 3,4-quinone form (E_1-3,4-Q and E_2-3,4-Q, resp., i.e. ultimate carcinogens) and guanine. (Free) energy of reaction was calculated as (free) energy of the product (adduct with guanine) minus (free) energy of reactants. All (free) energies are in kcal/mol.
a) B3LYP/6-31G(d) calculated gas phase energies.
b) B3LYP/6-31G(d) calculated zero point energy (ZPE) corrections. The ZPE was calculated as ZPE(product)-ZPE(reactants).
c) Free energy of hydration differences obtained using Langevin dipoles (LD) method with ChemSol 1.1 parametrization. Merz-Kollman charges were calculated using HF/6-31G(d) wavefunction (gas phase) applied to the B3LYP/6-31G(d) optimized geometry.
d) Free energy of hydration differences obtained using PCM solvent reaction field of Tomasi in conjunction with HF/6-31G(d) wavefunction.
e) LD free energy of hydration differences using ChemSol 2.1 parametrization, where Merz-Kollman charges were calculated at B3LYP/6-31G(d) level using Tomasi's PCM SCRF.
f) Reaction free energy $\Delta G_{react} = \Delta E + \Delta ZPE + \Delta G_{hydr}^{(e)}$. We feel that the LD method with ChemSol 2.1 parametrization is the most reliable.

No reactivity difference

No significant difference in reaction free energy for the reaction involving estrone and estradiol metabolites was found, **despite the fact that for the two substances different carcinogenic activities were reported**. Differences in carcinogenicity may be therefore attributed to other types of interactions or reactions such as (i) specific interactions of the carbonyl or hydroxyl group with DNA giving rise to different activation free energies for the reactions, (ii) the reaction of depurination and subsequent effects on the DNA, (iii) enzymatic or nonenzymatic oxidation steps (P450, aromatase, peroxidases, O2) and detoxification reactions (catechol-*O*-methyl transferase, S-transferase), or (iv) binding of the hormone to its nuclear receptors.

APPLICATION OF LFER TO THE STUDY OF THE REACTION BETWEEN BPDE AND GUANINE OR ADENINE.

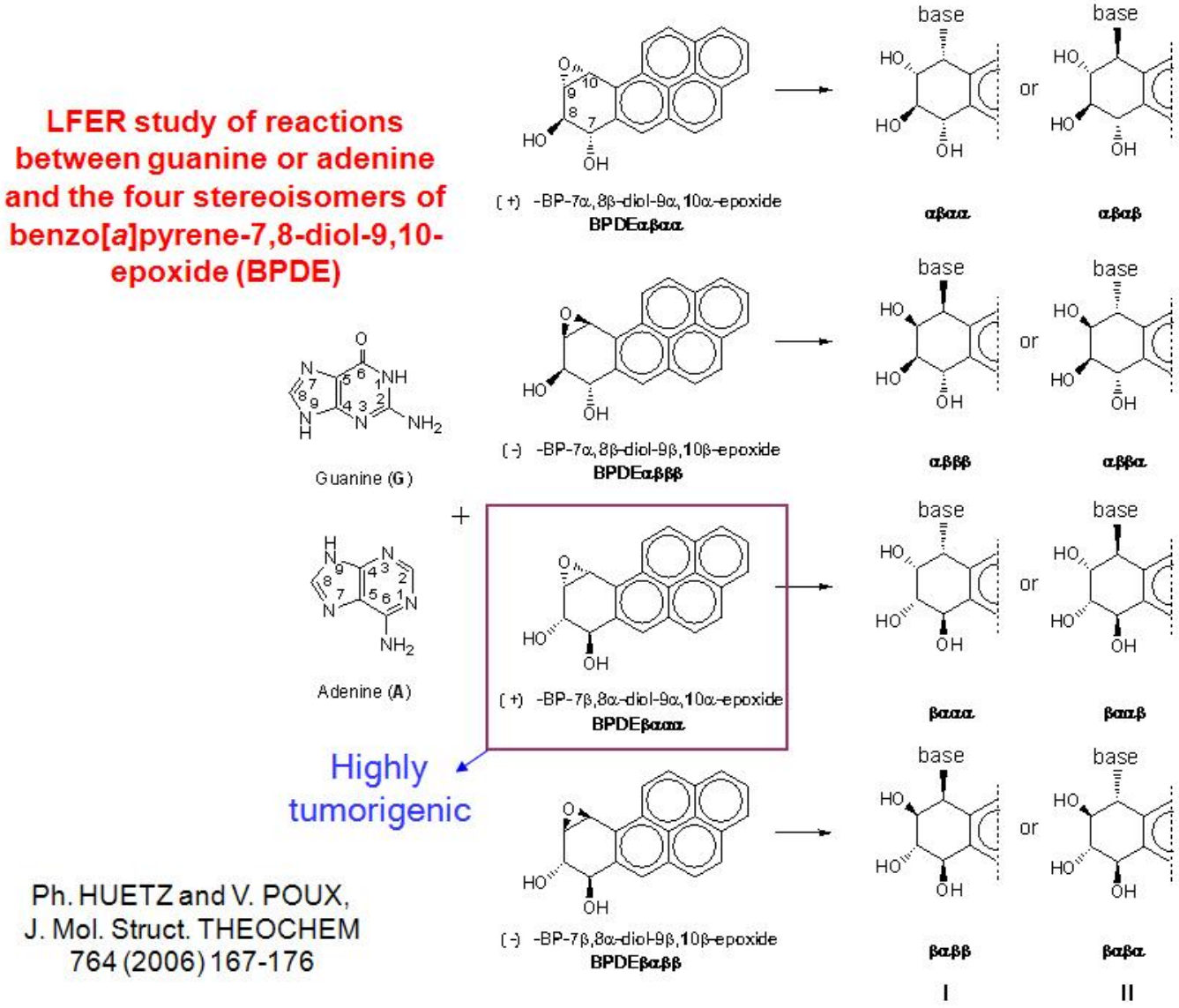

Despite the structural closeness of the four BPDE molecules (chemically identical but optically different), **BPDEβααα ((+)-7β,8α-dihydroxy-9α,10α-epoxy-7,8,9,10-tetrahydrobenzo[*a*]pyrene) was reported to be the most tumorigenic. Why ?** Using Linear Free Energy Relationships, what is possible because the four molecules are very structurally similar and the reaction mechanism with guanine or adenine is identical, we could compare activation free energies, extrapolated from the calculated free energies of reaction, exhaustively performing 32 free energy calculations.

RESULTS

Major adducts formed with BPDE according to literature →

Major adducts: **GE** > **AE**
Minor adducts: **GN**
Never reported: **AN**

(±) *anti*: *trans* opening (SN_1 or SN_2):
BPDEβααα → GEβααβ
BPDEαβββ → **GEαββα**

(±) *syn*: *cis* opening (SN_1):
BPDEαβαα → **GEαβαα**
BPDEβαββ → **GEβαββ**

Adduct	ΔE_{reac} PM3[a]	ΔE_{reac} B3LYP[b]	ΔZPE[c]	$\Delta\Delta G_{hydr}$ Tomasi[d]	$\Delta\Delta G_{hydr}$ LD[e]	ΔG_{reac} B3LYP Tomasi[f]	ΔG_{reac} B3LYP LD[g]
GEαβαβ	-31.73	-25.73	2.72	6.18	4.75	**-16.83**	**-18.26**
GEαββββ	-33.18	-22.29	1.92	5.61	4.46	-14.76	-15.91
GEβαααα	-34.22	**-31.38**	3.03	11.72	13.52	-16.64	-14.84
GEβαβα	-33.40	-23.80	2.25	5.55	7.73	-15.99	-13.81
GEαβαα	***-31.45***	***-22.03***	2.64	6.53	8.59	-12.85	***-10.79***
GEαββα	-33.39	-23.57	2.76	8.72	6.51	***-12.09***	-14.30
GEβααβ	**-37.34**	-24.35	2.19	7.19	8.20	-14.97	-13.96
GEβαββ	-34.08	-26.74	2.53	8.63	9.15	-15.59	-15.07
GNαβαβ	-28.74	-25.92	3.02	11.11	12.48	-11.78	-10.41
GNαββββ	-30.53	***-17.58***	2.33	7.51	7.37	***-7.74***	***-7.88***
GNβαααα	**-35.79**	-28.93	2.43	11.24	12.88	-15.25	-13.61
GNβαβα	-31.68	-23.76	2.22	7.92	9.14	-13.62	-12.40
GNαβαα	***-26.63***	-21.96	2.40	5.90	4.72	-13.66	-14.84
GNαββα	-30.99	-21.83	1.97	8.84	9.76	-11.02	-10.10
GNβαβ	-33.45	**-30.07**	2.36	11.79	12.61	-15.92	**-15.10**
GNβαββ	-32.67	-30.01	2.79	10.98	13.43	**-16.24**	-13.79
AEαβαβ	-35.40	-20.59	2.66	6.72	6.40	-11.21	-11.53
AEαββββ	-33.58	-22.25	2.29	4.94	3.16	-15.01	-16.79
AEβαααα	**-37.55**	**-32.51**	3.43	11.01	12.20	-18.07	-16.88
AEβαβα	-33.79	-24.32	2.75	5.56	7.38	-16.01	-14.19
AEαβαα	***-27.45***	***-19.48***	3.21	6.16	5.16	***-10.11***	***-11.11***
AEαββα	-33.89	-20.13	2.40	2.92	1.98	-14.81	-15.75
AEβαβ	-36.29	-30.85	2.86	8.15	7.97	**-19.84**	**-20.02**
AEβαββ	-34.66	-25.36	2.78	5.86	7.49	-16.72	-15.09
ANαβαβ	-27.50	-20.43	2.68	3.84	-0.97	-13.91	-18.72
ANαββββ	-26.63	-14.92	2.84	3.26	-1.73	-8.82	-13.81
ANβαααα	-30.65	-22.84	3.19	6.82	3.09	-12.83	-16.56
ANβαβα	-27.63	-20.43	2.68	3.85	-0.73	-13.90	-18.48
ANαβαα	***-24.16***	***-9.71***	2.69	1.37	-4.01	***-5.65***	***-11.03***
ANαββα	-24.88	-16.53	2.68	1.27	-6.64	-12.58	**-20.49**
ANβαβ	**-31.26**	**-26.52**	3.21	7.98	5.86	**-15.34**	-17.46
ANβαββ	-26.74	-20.41	2.72	3.37	-1.80	-14.33	-19.50

DFT (but not PM3) in contradiction with experimental values

Good correlation with experimental values

Adducts not observed experimentally
Possible solvent effect revealed here

Free energy and free energy components for reactions between each of the four stereoisomers of benzo[*a*]pyrene-7,8-diol-9,10-epoxide (BPDE) and guanine or adenine, at both N-cyclic and N-exocyclic positions of the bases.

All energies are given in kilocalorie per mole, and were calculated as energy of the adduct minus the sum of the energies of the reactants (stereoisomer + base).

G, A, E and N stand for guanine, adenine, *N*-exocyclic (reaction on position N^2 of guanine, N^6 of adenine) and *N*-cyclic (reaction on position N7 of guanine or adenine), respectively. α and β refer to the direction of hydroxyl bonds and bond with the corresponding nitrogen of the base, from positions 7 to 10 of the potential carcinogen.

[a] Gas-phase reaction energies (ΔE_{reac}) calculated at the semiempirical PM3 level.

[b] B3LYP/6-31G(d) calculated gas-phase energies.

[c] B3LYP/6-31G(d) ZPE corrections to the optimized structures obtained in b.

[d] Hydration free energy differences ($\Delta\Delta G_{hydr}$) determined using PCM SCRF at B3LYP/6-31G(d) level.

[e] Hydration free energy differences obtained using Langevin dipoles (LD) method with ChemSol 2.1 parametrization, Merz–Kollman charges being determined in PCM calculations.

[f,g] Reaction free energies: $\Delta G_{reac} = \Delta E_{reac}$ B3LYP + ΔZPE + $\Delta\Delta G_{hydr}$, the hydration term being issued either from PCM or from LD model. In bold normal: lowest values, in bold italics: highest values of a series.

Linear relationship between hydration free energy and total dipole moment of the molecules

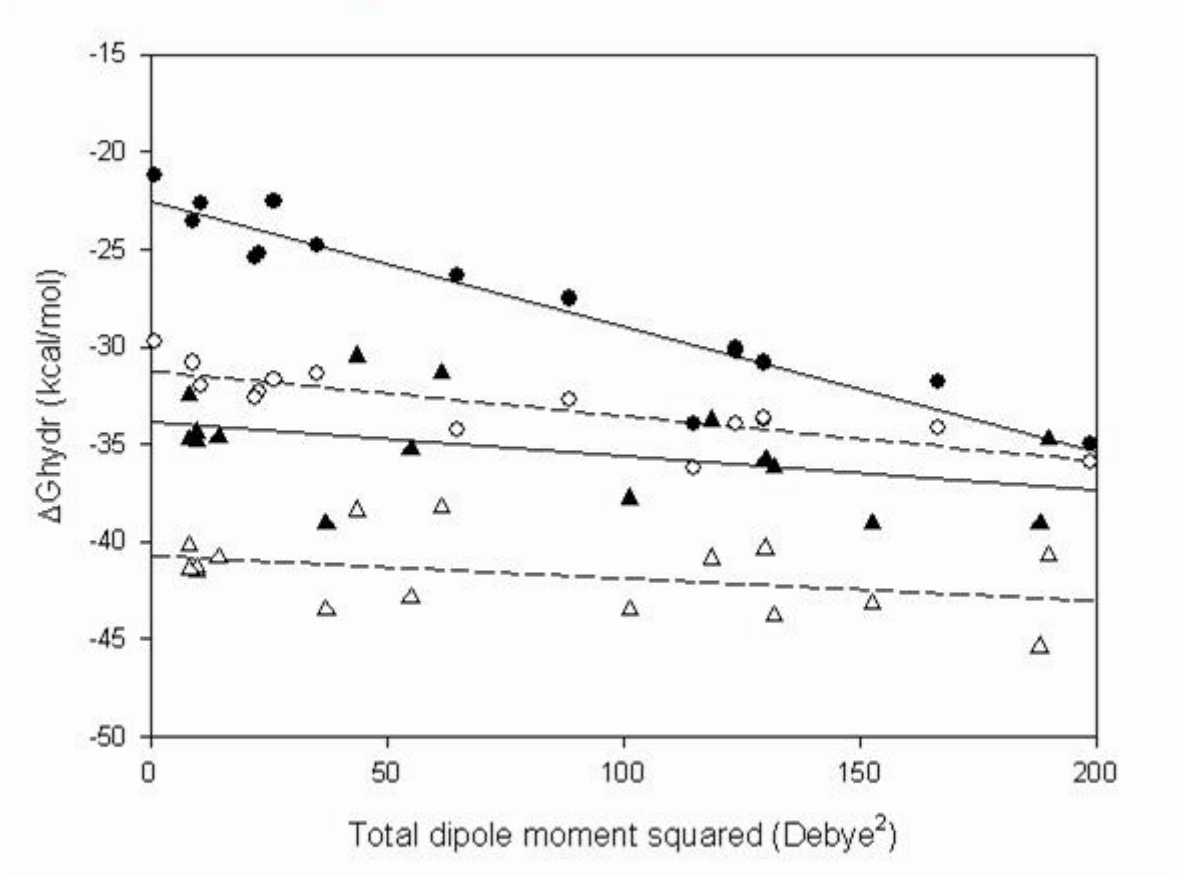

ΔG_{hydr} calculated with PCM (O, Δ) or LD (•, ▲) methods for both N-cyclic and N-exocyclic BPDE/adenine adducts (circles) and N-cyclic and N-exocyclic BPDE/guanine adducts (triangles) as a function of their total dipole moment squared (μTot^2)

BPDEβααα: anchimeric assistance ?

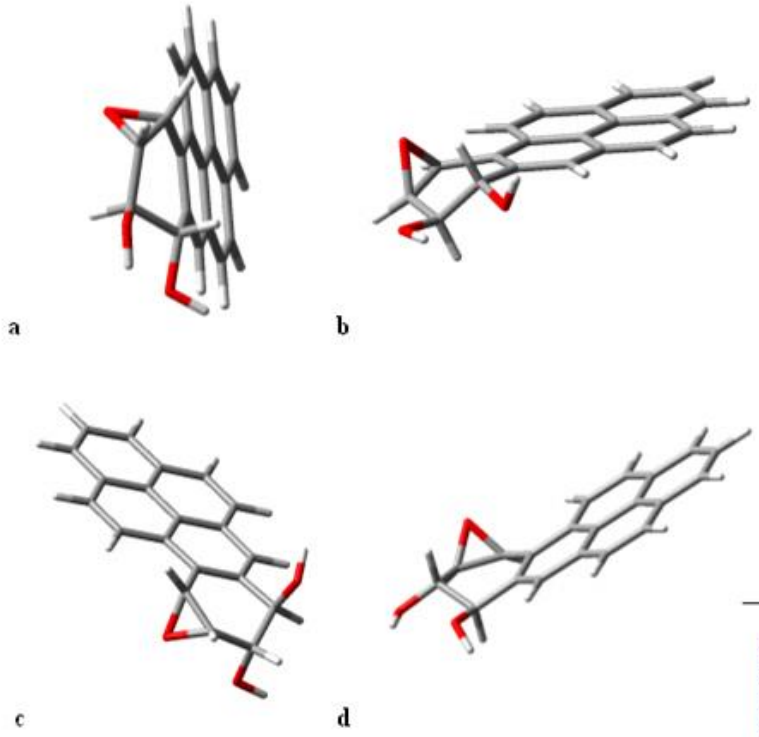

Reactant	ΔG_{hydr} PCM	ΔG_{hydr} LD
BPDEαβαα	-19.36	-16.54
BPDEαβββ	-19.04	-14.97
BPDEβααα	-22.56	-20.00
BPDEβαββ	-19.36	-16.63

B3LYP optimized isomers of BPDE
a) BPDEαβαα **b)** BPDEαβββ **c)** BPDEβααα **d)** BPDEβαββ

An important observation can be made when carefully looking at ΔG_{hydr} PCM and LD values. Indeed in the four BPDE isomers, BPDEαβαα and BPDEβαββ are enantiomers, as well as BPDEαβββ and BPDEβααα. But whereas for the first pair PCM and LD ΔG_{hydr}'s are identical, they are different for the second, with a pronounced difference in LD values. However, **enantiomers should have equal properties in non-chiral environment**: solvation free energies should be equal. The answer for this calculated difference is revealed in the figure, where the shown B3LYP optimized structures were used for ΔG_{hydr} evaluation. Indeed where hydroxyls are (pseudo)equatorial, hydration energies are comparable (slightly higher for BPDEαβββ), whereas for BPDEβααα, in which the 7-OH is axial, hydration energy is markedly lower.

We made the hypothesis that ***trans*** **anchimeric assistance** by the benzylic 7-hydroxy group **could enhance the reactivity of BPDEβααα**. This could be one plausible explanation accounting in an aqueous environment for the generally much higher in vivo mutagenicity and carcinogenicity observed for this particular isomer, even though solvent effects will have to be precised.

Modeling of chemical reactivity nowadays allows reliable predictions

- *in silico* evaluation of potential carcinogenicity of molecules
- Guide for the synthesis of anticarcinogenic molecules
- Calculate and predict chemical reactivity of different polyphenols. This includes about 4000 known flavonoids from natural substances

Chemical reactivity of these anticarcinogenic polyphenols must not be too high (phenol is highly toxic and mutagenic)

ULTIMATE AIM:

development of efficient anticarcinogenic molecules